Journal of Medical and oral biosciences
ISSN (Online): 3007-9551
ISSN (Print): 3007-9543

JMOB
Open Access DOAJ

Type: Research article
Published: 18/ 11/2024

Ultrasonic Processor effects on the nanoscale of MgO Nanoparticles and Assessing its Antibacterial activity Before and After Treatment

Zainab J. Shanan [1], Rand A.Hayder [2 *a], , Sarab. Murad [3b], and Ali Saeed Jassim [4]

[1] Department of Physics, College of Science for Women, University of Baghdad, Baghdad, Iraq
https://orcid.org/0000-0002-5166-5200
[2, 3] Department of basic Science, College of Dentistry, Al-Iraqia University, Baghdad, Iraq
[a] https://orcid.org/0009-0001-4359-9506
[b] https://orcid.org/0009-0002-9685-0490
[4] Department of Geology, Faculty of Science, University of Kufa Al-Najaf, Iraq,
https://orcid.org/0000-0001-8659-2497

OPEN ACCESS

ARTICLE INFO
Received: 16/ 10/2024
Revised: 30 / 10/ 2024
Accepted: 8 / 11/2024
Publish online: 18/11/2024

* Corresponding Author: Rand A. Hayder
Email: rand.a.hayder@aliraqia.edu.iq
https://orcid.org/0009-0001-4359-9506

CITATION

Zainab J. Shanan. , Rand A Hayder , Sarab Murad and Ali Saeed Jassim. (2024). Ultrasonic Processor effects on the nanoscale of MgO Nanoparticles and Assessing its Antibacterial activity Before and After Treatment. JMOB. 1;(4): 44-56.
https://doi.org/10.58564/jmob.67

Abstract

Quinoa seed extract functioned as reducing agent in synthesis of magnesium oxide nanoparticles by using green method. In this work, an ultrasonic probe was employed for decreasing the particle size and control the (Eg) energy gap, which was reported to be 4.9 eV and was actually 4.5 eV. The grain size of the MgO nanoparticles was found to be 51.03 nm by morphological analysis; however, ultrasound reduced it to 38.67 nm, the average particle size was determined by field emission scanning electron microscopy examination to be 13.96 nm. The particle morphology was almost spherical with sponge-like properties. The antimicrobial activity of the synthesized magnesium oxide nanoparticles and micro-magnesium oxide nanoparticles was measured using ultrasound. The MgO NPs showed effectiveness at a lower concentration of inhibiting agents with (500) µg/mL MgO NPs. Ultrasonication had a better effect on MgO NPs. It looks like this.

Keywords: MgO nanoparticles, green methods, ultrasonic, positive bacteria, AFM, and (MIC)

Introduction

In the last years, many of nanoparticles oxides synthesis with high reactivity and with large surface areas has been registered (1). Metal oxides are interesting because they are safe materials for humans and animals such as ZnO, TiO_2, CaO and MgO (2). The properties of synthesized nanoparticles are mostly determined by crystalline, size, composition, shape, and morphology (3). Several synthesis methods have been reported for the production of MgO:

liquid phase, vapor-phase, gas-phase (4). But in this research, we presented the analysis in the green method. MgO is required in the environment, health products, and industry (5) . MgO is used as antibacterial agent includes oxidative stress and membrane damage, which prevents bacteria from functioning and reproducing. (6). Magnesium oxide nanoparticles exhibit antimicrobial activity against various microorganisms, especially bacteria.(7),which need to be focused and studied on different levels. *Quinoa* grain is defined as an amylaceous material has a high-carbohydrate content that is mainly made up of starch and a few percentage sugars. It also contains vitamin C and E, fiber and minerals like magnesium , calcium, potassium, iron , phosphorus, sodium, manganese, zinc, and copper (8-12). *Quinoa* seeds is a plant has adaptable to climatic conditions and different kinds of soil, hence raised the attention of the scientific community being rich in proteins, dietary fiber, minerals and vitamins, their nutritional value is unsaturated fat with a gluten-free that can be used for gastrointestinal disorders in patients' diets (9, 13). Plants produce many organic compounds which have antibacterial activity (14). The main constituents Which make effective antimicrobials involve saponin, flavonoids, thymol, phenol, cholesterol, linalol, terbene and their precursors (15). Flavonoids, phenols, and saponins were identified as biologically active ingredients of *Quinoa* seeds (13, 16). Ultrasound is one of the vigorous techniques in the application and synthesis of nanomaterials. Normally, ultrasonic cavitation in liquids results in degassing that can be both rapid and complete; it enhances chemical reactivity due to better mixing of reactants, polymerization reactions, and depolymerizes by breaking the chemical bonds in the polymer chains (17). Ultrasound has a wide range of applications (in (physical, biological, and chemical) processes. Most applications of high-intensity ultrasound exploit a cavitation effect (18). The aim of the study is to investigate the antibacterial activities of both nanoparticles and mini-nanoparticles of MgO-NPs through an ultrasonic processor.

Methodology

Green Biosynthesis of MgO-NPs

Preparation extract of the *Quinoa* seeds.

Seeds of Iraqi origin were acquired from the Department of Agriculture, /University of Baghdad. These were washed with water to remove adhering impurities and then with distilled water several times. Finally, they were dried in hot air oven at 40 °C until constant weight and powdered with an electric grinder to get a soft powder of Quinoa seeds. The (15) gm of powdered seeds were thoroughly extracted with (200)ml of boiling (DW) distilled water through homogenization with the (magnetic stirrer) for approximately an hour. The product solution obtained after final filtration was concentrated in a rotary vacuum evaporator, lyophilized, and stored at 4°C for further analysis.

Biosynthesis of MgO-NPs utilizing extract of the *Quinoa* seeds.

Forty milliliters of the aqueous seed extract from *Quinoa* were magnetically stirred and heated to 60 °C when 40 ml of magnesium nitrate solution with concentration 0.1 M was slowly added while keeping it continuously stirring at 1500 rpm. The temperature was allowed to stabilize for 3 min before 2M NaOH was added dropwise to attain a pH range of 10-12 on a color change. It forms Mg(OH)2 which is shown in the solution in a while after the alkalinity solution has been added. The whole process was maintained for 2 hours, causing the solution to change color to lemon yellow (as displayed below in Figure (1).

(a) (b)

Figure. 1: MgO Nanoparticles by Bio green-method. (a) Magnesium salt solution with plant extract before adding (NaOH) (b) change to yellow solution -after adding (NaOH)

After that, it was centrifuged for 15 minutes at 4000 rpm. The precipitate that resulted was then heated to 400 °C for three hours. Eventually, the material was gathered and recognized as a white powder, as illustrated in Figure.2 below. It was then preserved for further analysis.

Figure.2: Synthesized MgO- nanoparticles(white powder).

This method was used to prepare 0.1 mg of MgO NPs. The synthesised MgO NPs were dispersed in 100 milliliters of distilled water to create the sample. Next, it was moved to a 750 Watt, 20 kHz ultrasonic processor device. The instrument was operated for 5 days for 1 1/2 hours per day (10 seconds of work and 5 seconds resting). X-ray diffraction helps in grain size, which depicts the crystalline nature of the material and from the XRD pattern grain size was evaluated. UV absorption studies show that as the size of the particle reduces, the absorption of UV radiation by nanoparticles increases. X-ray absorption is because of the excitation of electrons in a material. This research, focused on optimizing the synthesis of MgO nanoparticles via combustion methods, set out by an easy synthetic route since that was its very purpose.

Antibacterial activity study

Preparing bacterial culture/ Minimal Inhibitory Concentration (MIC)

Sub-culturing two bacterial strains in Nutrient Broth and incubating them for 18 hours at 37 °C were provided by the Biology Department at the University of Baghdad. Following that, every strain of bacterial stock solution was utilized in other studies. By using the MIC investigation in the microtiter polystyrene plate of ninety-six flat-bottomed wells, antibacterial activity for MgO at the nanoscale was also investigated against pathogenic bacteria of both Gram-positive *(S. aureus*) and Gram-negative (*E. coli*) kinds. Fresh

Bacterial subcultures were prepared prior to the experiment via inoculating bacteria within a 10 mL nutrient broth test container and incubated at 37 °C for 18 hours. The different concentrations of MgO NPs (250 µg/ml , 500µg/ml , 1000µg/ml , and 2000 µg/ml) were studied. 100 µl of each concentration of MgO-NPs was prepared in a manner described for bacterial growth in each well of the microtiter plate after resuspending in 1.5*10^8 cells/ml, 0.5 MacFarland turbidity. MIC, thus is the lowest MgO NPs concentration at which no growth is detected. Volumes of 100 µl bacterial culture at MIC, the previous higher concentration, is next transferred and streaked onto sterilized Nutrient Agar plates thereafter incubated at 37 º C for 24 hr. Minimal Bactericidal Concentration (MBC) was thus defined as the lowest concentration of MgO NPs that eliminated 100% of the bacteria (20). The resazurin microplate assay was carried out by adding 20 µL of a 0.01% (w/v) resazurin sodium salt solution in Milli-Q water to each well, using a repeating pipette. The plates were then incubated as explained above. After the defined period of incubation, i.e. 2–4 h, bottom readings were recorded. It was recorded at an excitation wavelength of 530–540 nm and at emission of 590 nm bottom readings using a fluorescence multimode plate reader.

Resazurin Microplate Assay

To each well of the plate, 20 µL of 0.01% (w/v) solution of resazurin sodium salt in Milli-Q water was added, using a repeating pipette. The plates were then kept for incubation in the same manner as described for MTT assay. After the specified period of incubation, that is, 2–4 h, measurements of fluorescence were done. Measurements of readings from the bottom were done at an excitation wavelength of (530–540) nm and an emission wavelength of 590 nm by means of a fluorescence multimode plate reader. The test was performed using the broth microdilution method with some modifications as described by Coban (2012)(21) with some modifications. In-vitro Resazurin assay NPs were aseptically transferred Resazurin powder to the wells, and Fifty µL of sterile nutrient broth was added to each of the first six wells, MgO NPs were introduced to the first three wells in a two-row configuration for the ultrasonic MgO NPs and to wells four through six in a two-raw configuration to ultrasonic untreated MgO-NPs. Bacterial suspension at 5 µl(equivalent to 0.5 of a MacFarland turbidity standard approximately 1.5*108 cell/ml transferred into every of the previous wells (First row exhibiting growth of *Escherichia coli* and second row exhibiting development of *Staphylococcus aureus)*. The dish plate was sealed with parafilm and placed in a plastic bag with a damp paper towel. The bag is closed but not sealed to avoid dehydration of wells. The bag then loosely put in the incubator and incubated aerobically at 35C for 18hr. After incubation, 15 µl of stock dye solution was added to all the wells of the broth microdilution plate using an electronic multichannel dispenser and mixed properly. The plates reintubated at 37 C temperature for 75 more minutes. If live bacterial cells are present, then the blue color will go to pink. Otherwise, dead or inhibited bacterial cells will remain blue or purple in color.

Results and discussion

X-ray Diffraction

XRD pattern of the synthesized MgO powder is shown in Figure (3). It confirms that the crystalline system for the synthesized MgO is cubic. The 2θ peak positions well agree with standard data having (JCPDS NO: 00-045-0946). crystalline nano- size was also evaluated by the Debye Scherrer's formula

$$D = 0.94\lambda/\beta \cos\theta$$

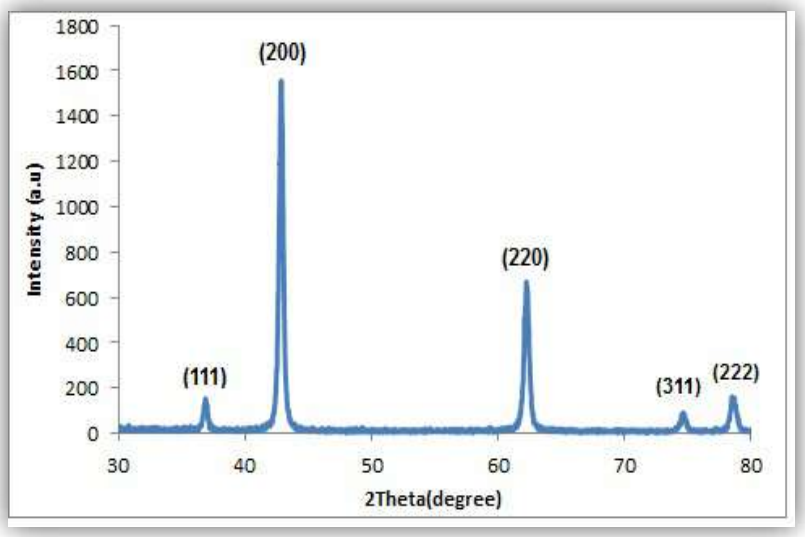

Figure. 3: XRD Analysis for MgO-NPS

The estimated size of the crystals formed by the synthesis of both the MgO-Nps is smaller than the Table's depiction of the system's quantum confinement. This outcome compatible with previously reported studies done by EL-Moslamy *et al*., 2018 and Balraj *et al.,* 2018 (22, 23). The estimated size of the crystals in the system of quantum confinement was used to calculate the estimated size of the syntheses MgONPs. This demonstrates that NPs were produced in the QC. The confinement of quantum system as outlined in Table (1). Other impurities in the manufactured nanopartides and the sharp peaks that define the nature of the material indicate that it is essentially crystamne.

Table.1: Shows(D) crystalline size for- MgO-NPs

2θ (Deg.)	**FWHM (Deg.)**	**Crystalline size D(nm)**	**hkl**
36.936	0.0066	21.11	(111)
42.9158	0.0064	21.80	(200)
62.3021	0.0042	34.18	(220)
74.6889	0.0071	20.59	(311)
78.6278	0.0067	21.71	(222)

Optical analysis

The UV-VIS absorption spectrum (24). Absorption spectra of a MgO NPs before and after treatment with Ultrasonic Processor are shown in figures (4),and (5) recorded within the wavelength of (200-800). It was noticed from these figures that the edge of optical absorption at 252 nm (before the treatment) changes to an absorption peak at 270 nm (after treatment), shifted to higher wavelengths after treatment with the ultrasonic processor, which in turn reduces the E_g energy gap from 4.9 eV to 4.5 eV. This outcome was in good agreement with previously reported observations of Renata, (2016) (25). The strong absorption of metal oxide nanomaterials is in the UV-VIS region, which proves suitability regarding this product for medical applications such as solar screen protectors or as an antiseptic in ointments (26). The energy band gap (Eg) of the synthesized MgO NPs was calculated by the formula: $E= hc/\lambda$

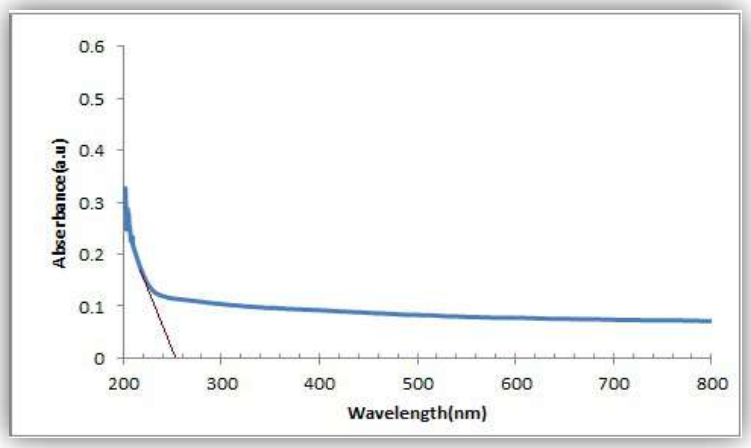

Figure. 4: UV–Visible analysis for the production of MgO nanoparticles before ultrasonic treatment

The energy gap in bulk MgO has been seen to reduce from 7.8 eV to 4.9 eV and 4.5 Ev before and after treatment, with the shift in wavelength perhaps being caused by an increase in MgO NP aggregation. This occurs due to the defects accompany by the manufacturing of MgO nanoparticles (9, 22).

Atomic Force Microscopic (AFM) study

Atomic Force Microscopic (AFM) the word "microscopic" provides a microscopic description that makes it easier to create topographic maps that show the surface's structure and height. This method applies photographs allow for the quantitative assessment of a surface characteristics, such as mean roughness (Ra) and mean square root roughness (Rq), as well as image analysis from multiple perspectives, including 3D simulation (27). Figures (6) and (7) observe 3D (AFM) images with granularity accumulation distribution for MgO-NPs with and without use of the processor, which notes that, the most of the particles were spherical and the few were cylindrical and with grain size of 51.03 nm before use the processor of the ultrasounds and become spherical after treatment with grain size of 38.67nm

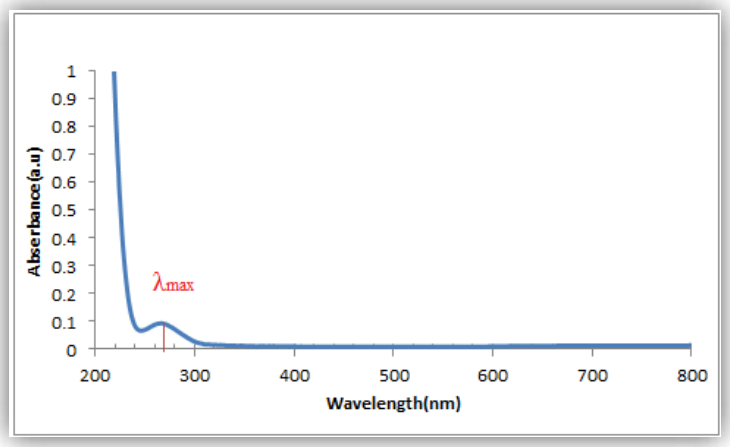

Figure. 5: UV–Visible analysis for the production of MgO nanoparticles after ultrasonic treatment.

Atomic Force Microscopic (AFM) study

Atomic Force Microscopic (AFM) the word "microscopic" provides a microscopic description that makes it easier to create topographic maps that show the surface's structure and height. This method applies photographs allow for the quantitative assessment of a surface characteristics, such as mean roughness (Ra) and mean square root roughness (Rq), as well as image analysis from multiple perspectives, including 3D simulation (27). Figures (6) and (7) observe 3D (AFM) images with granularity accumulation distribution for MgO-NPs with and without use of the processor, which notes that, the most of the particles were spherical and the few were cylindrical and with grain size of 51.03 nm before use the processor of the ultrasounds and become spherical after treatment with grain size of 38.67nm.

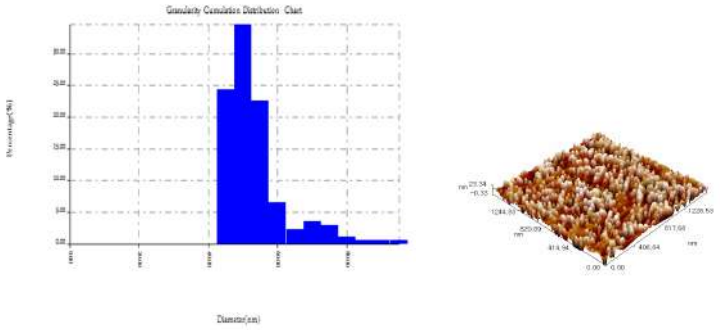

(a) (b)

Figure. 6: AFM images(a): 3D , and (b): the granular distribution of MgO NP_s synthesized by the aqueous extract of *Quinoa* seeds by green method before treatment by ultrasonic.

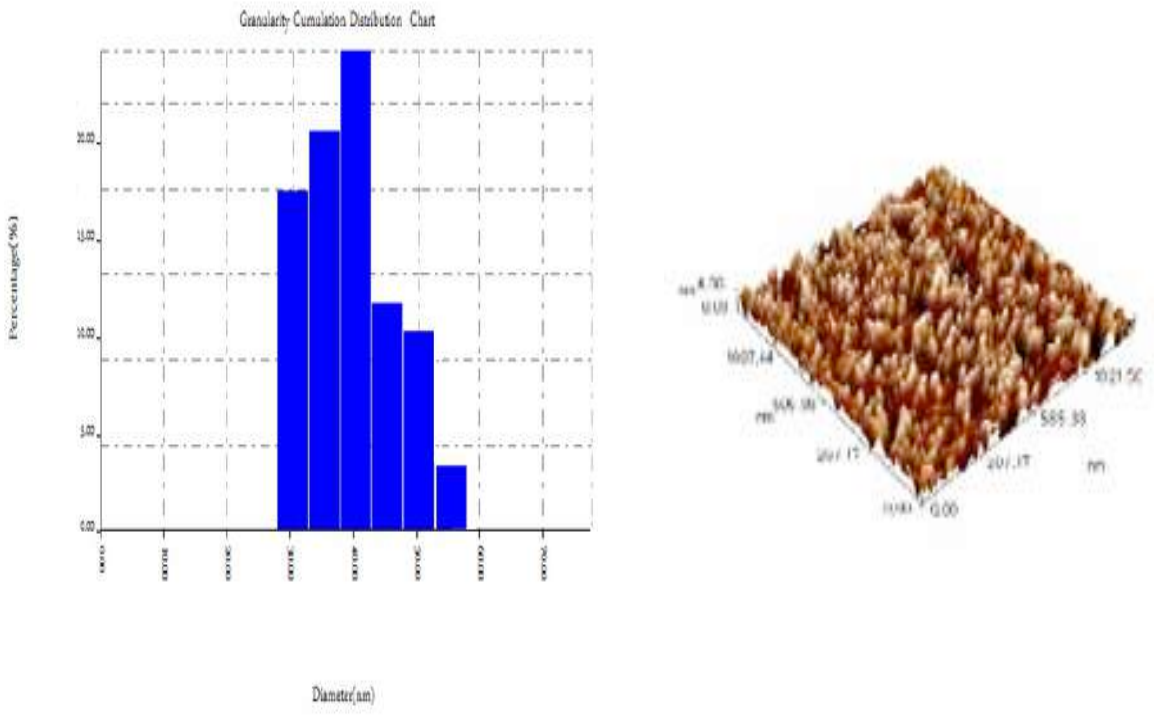

(b) **(a)**

Figure. 7: AFM images (a) 3D,(b): the granular distribution of MgO NP_s synthesized by the aqueous extract of *Quinoa* seeds by green method after treatment by ultrasonic.

It can be seen that the nanoparticles after ultrasonic treatment were obtained a homogeneous nano fluid with decrease size of MgO nano particles with a homogeneous distribution.

Field Emission-Scanning Electron microscopy (FE-SEM) study.

Figure. 8 and 9) show FE-SEM images of synthesized MgO NPs from the aqueous extract of *Quinoa* seeds by green method before and after using the ultrasonic processor. It is obvious from (8) images, that the forms of morphology in MgO nanostructures is a porous, spongy containing a conjunctive granular structure with an average size of 19.15 nm .

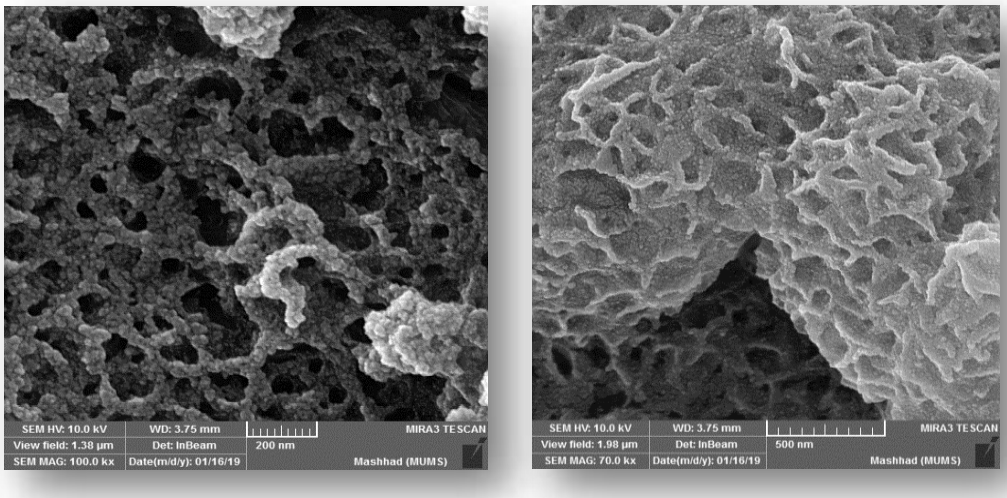

Figure. 8: Shows the surface morphology of MgONPs synthesized by the aqueous extract of *quinoa* seeds by FE-SEM

After using the ultrasonic processor the effects on MgONPs was observed by changing the particle size from 19.15 nm to 13.96 nm with change the shape to the spherical nano shape and with homogeneous uniform distribution as shown in figure (9) these results agree with AFM images.

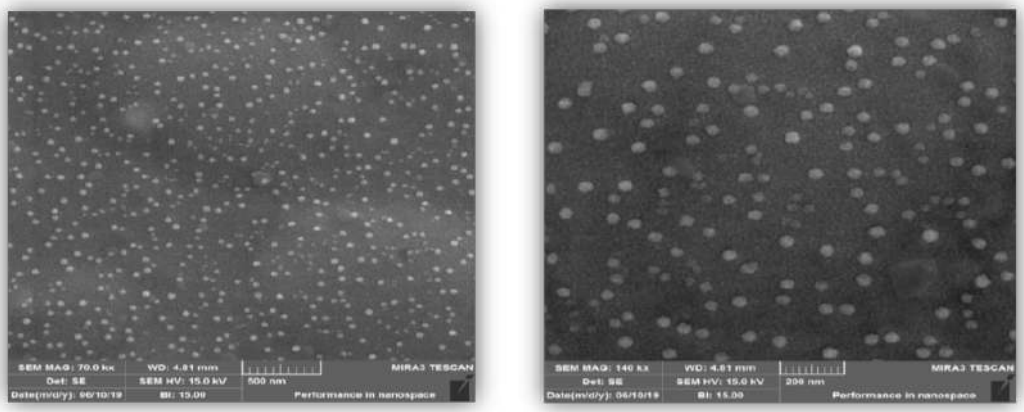

Figure (9): Shows the surface morphology of MgO NPs synthesized by the aqueous extract of Quinoa seeds By FE-SEM processed by ultrasonic.

Antibacterial activity

Antibacterial activity Using (MIC)assay

In this research, the pathogenic bacteria *S. aureus* and *E. coli* were shown to be susceptible to the antibacterial activity of MgO NPs, and after ultrasonic processing, the minimum inhibitory concentration (MIC) of MgO NPs for both of them was 500 µg/ml, however, without ultrasonic processing, MgO NPs had no effect on E.coli at any concentration (2000 µg/ml). However, it demonstrated the same effect on *S.aureus* at 500

µg/ml. The MgO NPs, as a whole, have a general antibacterial effect (22,23). The green synthesis of nanoparticles is considered superior to other chemical methods in several regards. The current research that is discussed below concerns the utilization of *Qiunoa's* extract seeds in the synthesis of green NPs that have a slower propensity to act against *S.aureus* bacteria; this is believed to be due to the different cellular walls between the types of *S.aureus* and *E.coli*' (24,25). In the current study, one of the main reasons for the accompanying mortality brought on by the breakdown of the cell membrane could be the existence of active (O_2)oxygen, like superoxide, on surface of the produced MgO-NPs. Because ultrasonic treatment can keep the particles floating and dispersed in a suspension instead of as an inert sediment, the results obtained also show the beneficial effect of ultrasonic treatment of the MgO- NPs to the growth of the bacteria.Ultimately, ultrasound is compromised by the demands of energy expenditure and the increasing degree of powder division. As a result, the MgO NPs are more effective against the pathogenic bacteria developing in the broth's suspension .

Microdilution Assay(Resazurin)Test

The activity of Resazurin against bacteria was employed as a means of verification (indicator of growth) of the(MIC) assay. Bacterial cells were observed in the 250 µg/ml treated wells regarding *Escherichia coli* and *Staphylococcus aureus* during 75 minutes of incubation, as can be seen in (Figure 10).

Figure (10). Plate after 75 minutes. Resazurin test {The pink hue signifies growth, while the blue hue denotes growth inhibition]

Only after being incubated with nanoparticles at (500 µg/ml), nonviable cells were observed (a purple color) when processing samples at 2000 and 1000 µg/ml, all of the cells were nonviable (a blue color). The increase in size was inhibited greatly when bacterial cells were incubated with MgO NPs that were ultrasonicated at a concentration of (1000) µg/ml. Based on this examination**,** it was recorded that the growth of *S. aureus* was very low after being incubated with (500 µg /ml, 1000 µg/ml , and 2000 µg/ml)of MgO NPs

,the quantity of dead cells escalated with the concentration of 2000 µg/ml and 1000 µg/ml of MgO nanoparticles using the ultrasonic mixer., in comparison to the control and *E. coli*. The information obtained is similar to the MIC method, this outcome suggests that resazurin is a viable candidate for use in the assessment of the antibacterial efficacy of several nanoparticle materials, because other methods, such as plant extracts and essential oils, have been employed in different situations

Conclusion

The present study reports the biological synthesis and sonication size reduction of MgO NPs antibacterial agents. XRD patterns confirm the crystalline nature of magnesium oxide with a cubic phase. The crystal size was calculated to be about 20.59 nm. Analysis of FESEM images shows before ultrasonic treatment the MgO NPs were spongy in nature. The particle size was reduced upon sonication and changed to spherical-shaped particles with a crystal size of 13.96. The MgO NPs demonstrated MIC at a lower inhibiton concentration with 500 µg/ml , having an improved outcome for the ultrasound-treated sample.

DECLARATIONS

Acknowledgments

We would like to thank the College of Science for Women, Department of Physics and College of Science, Department of Biotechnology, University of Baghdad for supporting this research.

Funding
There is no source of funding

Competing interests statement

No conflict of interest related with the publishing of this article.

Ethics statement

The author approved that this research follows the journal's Attach Ethic Approval guidelines as appeared on the journal's author guidelines page.

References

1. Camtakan Z, Erenturk SA, Yusan SD. Magnesium oxide nanoparticles: preparation, characterization, and uranium sorption properties. Environmental Progress & Sustainable Energy. 2012;31(4):536-43.
2. Stoimenov PK, Klinger RL, Marchin GL, Klabunde KJ. Metal oxide nanoparticles as bactericidal agents. Langmuir. 2002;18(17):6679-86.
3. Dickson RM, Lyon LA. Unidirectional plasmon propagation in metallic nanowires. The Journal of Physical Chemistry B. 2000;104(26):6095-8.
4. Agrawal R, Charpe S, Raghuwanshi F ,Lamdhade G. Synthesis and characterization of magnesium oxide nanoparticles with 1: 1 molar ratio via liquid-phase method.

International Journal of Application or Innovation in Engineering & Management. 2015;4(2):141-5.
5. Kantam ML, Pal U, Sreedhar B, Choudary BeM. An efficient synthesis of organic carbonates using nanocrystalline magnesium oxide. Advanced Synthesis & Catalysis. 2007;349(10):1671-5.
6. Leung YH, Ng AM, Xu X, Shen Z, Gethings LA, Wong MT, et al. Mechanisms of antibacterial activity of MgO: non-ROS mediated toxicity of MgO nanoparticles towards Escherichia coli. Small. 2014;10(6):1171-83.
7. Sundrarajan M, Suresh J, Gandhi RR. A comparative study on antibacterial properties of MgO nanoparticles prepared under different calcination temperature. Digest journal of nanomaterials and biostructures. 2012;7(3):983-9.
8. Filho AMM, Pirozi MR, Borges JTDS, Pinheiro Sant'Ana HM, Chaves JBP, Coimbra JSDR. Quinoa: nutritional, functional, and antinutritional aspects. Critical Reviews in Food Science and Nutrition. 2017;57(8):1618-30.
9. Alvarez-Jubete L, Auty M, Arendt EK, Gallagher E. Baking properties and microstructure of pseudocereal flours in gluten-free bread formulations. European Food Research and Technology. 2010;230(3):437.
10. Jancurová M ,Minarovičová L, Dandar A. Quinoa–a rewiev. Czech Journal of Food Sciences. 2009;27(2):71-9.
11. Spehar CR, Santos R, Veloso R. Quinoa: alternativa para a diversificação agrícola e alimentar. Planaltina: Embrapa Cerrados. 2007;1.
12. James LEA. Quinoa (Chenopodium quinoa Willd.): composition, chemistry, nutritional, and functional properties. Advances in food and nutrition research. 2009;58:1-31.
13. Alvarez-Jubete L, Wijngaard H, Arendt E, Gallagher E. Polyphenol composition and in vitro antioxidant activity of amaranth, quinoa buckwheat and wheat as affected by sprouting and baking. Food chemistry. 2010;119(2):770-8.
14. Ruiz KB, Biondi S, Oses R, Acuña-Rodríguez IS, Antognoni F, Martinez-Mosqueira EA, et al. Quinoa biodiversity and sustainability for food security under climate change. A review. Agronomy for sustainable development. 2014;34(2):349-59.
15. Juneja VK, Dwivedi HP, Yan X. Novel natural food antimicrobials. Annual review of food science and technology. 2012;3:381-403.
16. Hassan S, Haq A, Byrd J, Berhow M, Cartwright A, Bailey C. Haemolytic and antimicrobial activities of saponin-rich extracts from guar meal. Food Chemistry. 2010;119(2):600-5.
17. Kuldiloke J. Effect of ultrasound, temperature and pressure treatments on enzyme activity and quality indicators of fruit and vegetable juices. 2002.
18. Hielscher T. Ultrasonic production of nano-size dispersions and emulsions. arXiv preprint arXiv:07081831. 2007.
19. Das B, Moumita S, Ghosh S, Khan MI, Indira D, Jayabalan R, et al. Biosynthesis of magnesium oxide (MgO) nanoflakes by using leaf extract of Bauhinia purpurea and evaluation of its antibacterial property against Staphylococcus aureus. Materials Science and Engineering: C. 2018;91:436-44.
20. Janthima R, Khamhaengpol A, Siri S. Egg extract of apple snail for eco-friendly synthesis of silver nanoparticles and their antibacterial activity. Artificial cells, nanomedicine, and biotechnology. 2018;46(2):361-7.
21. Coban AY. Rapid determination of methicillin resistance among Staphylococcus aureus clinical isolates by colorimetric methods. Journal of clinical microbiology. 2012;50(7):2191-3.

22. EL-Moslamy SH. Bioprocessing strategies for cost-effective large-scale biogenic synthesis of nano-MgO from endophytic Streptomyces coelicolor strain E72 as an anti-multidrug-resistant pathogens agent. Scientific reports. 2018;8(1):3820.
23. Balraj B, Senthilkumar N, Potheher IV, Arulmozhi M. Characterization, antibacterial, anti-arthritic and in-vitro cytotoxic potentials of biosynthesized Magnesium Oxide nanomaterial. Materials Science and Engineering: B. 2018;231:121-7.
24. Smitha S, Nissamudeen K, Philip D, Gopchandran K. Studies on surface plasmon resonance and photoluminescence of silver nanoparticles. Spectrochimica Acta Part A: Molecular and Biomolecular Spectroscopy. 2008;71(1):186-90.
25. Dobrucka R. Synthesis of MgO nanoparticles using Artemisia abrotanum herba extract and their antioxidant and photocatalytic properties. Iranian Journal of Science and Technology, Transactions A: Science. 2.55-547:(2)42;018
26. Anantharaman A, Sathyabhama S, George M. Green synthesis of magnesium oxide nanoparticles using Aloe Vera and its applications. International Journal for Scientific Research and Development. 2016;4(9).
27. Al-Rasoul KT, Abbas NK, Shanan ZJ. Structural and optical characterization of Cu and Ni doped ZnS nanoparticles. Int J Electrochem Sci. 2013;8(4):5594-604.